ETH
Eidgenössische Technische Hochschule Zürich
Swiss Federal Institute of Technology Zurich

TIK Institut für Technische Informatik und Kommunikationsnetze

Master Thesis
at the Department of Information Technology
and Electrical Engineering

Thermal Energy Scavenging for WSNs

FS 2015

Dominik Böhi

Advisors: Dr. Jan Beutel
Reto Da Forno
Professor: Prof. Dr. Lothar Thiele

Zurich
September 23, 2015

Abstract

This work investigates the possibility of using thermal energy scavenging to power wireless sensors which are used in the Permasense project at ETH Zurich. These sensor are currently battery powered, which means that regular maintenance is required. As the sensor are located in hard to reach, high alpine regions, this is very expensive. Thermal energy scavenging using naturally occurring temperature gradients could offer a solution.

To explore this, a model is proposed which is able to estimate the amount of energy harvested at different positions, based on temperature data collected during the last years. Based on initial results from this model, a prototype system was designed and evaluated, to offer an initial evaluation of the feasibility of using thermal energy scavenging in the Permasense project.

Acknowledgements

First, I would like to thank my advisor, Dr. Jan Beutel, for his invaluable help in completing this thesis.

Further, I appreciate the great support from Felix Sutton during the layout of the prototype circuit board. I also thank Moritz Thielen, from the Micro and Nanosystems group at ETH, for his support in regard to all questions concerning thermal energy harvesting.

Finally, I would like to express my gratitude to Prof. Dr. Lothar Thiele for the opportunity to work on such an interesting project in his group.

Contents

Tables

Figures

1

Introduction

1.1 Motivation

Wireless sensor networks (WSNs) are becoming more popular with the advent of cheaper and more efficient sensors. Most networks still rely on battery power, which means that their lifetime is inherently limited, although technological advantages now allow runtimes of several years. While this is sufficient for a lot of case, this poses a problem when measurements of slow-changing, long-term effects are desired. Periodic maintenance is a possible solution to this, but is not always feasible. It increases the operating cost of the system, and requires the possibility of being able to access the system to change batteries. For sensor networks used in hard to reach environments, or environments not reachable at all, this is not a satisfying solution. Energy scavenging on the other hand is a promising solution allowing potentially unlimited operation, only limited by external influences or age related failure of the components. It can also open up new possibilities, by allowing the use of sensors with higher power requirements, which might no be usable with battery power.

But energy scavenging also several disadvantages. It is dependent on energy available in the environment, and cannot offer the same reliability as a power supply using a battery. The dependency on the environment also makes the system less predictable. This problem is increased by the usually low amount of energy which can be harvested.

The Permasense project runs several sensor networks in high alpine areas, which are currently battery powered. The use of energy scavenging could possibly remove the necessity to use batteries at all, or at least improve the runtime of the existing solution. A common technology for power generation are solar cells. Unfortunately, the location of the sensors in a high alpine area makes it difficult to use solar power generation. The individual sensor are often located at positions without direct solar irradiation, which limits the power which can be harvested. The location in areas prone to rockfall also means that solar cells are to fragile to be used without significant protection.

As an alternative to solar energy harvesting, we will investigate the use of thermal energy harvesting. It is possible with small and robust generators, and not as dependent on solar irradiation, which offers promise for the operation in a high alpine environment.

1.2 Contribution

This work contributes:

- Analysis of the requirements for a thermal energy harvesting system
- Characterization of the temperature gradients at the deployment region
- Design and evaluation of a prototype system

1.3 Related work

The use of energy harvesting to power wireless sensor nodes is an active research area. [1] gives an overview over the main energy sources which are under investigation.

Most of the work regarding thermal energy harvesting is done in industrial environments, where sensors in hard to reach locations are powered using temperature differences occurring due to waste heat produced by motors and other machinery [2]. In these applications, the available temperature difference is in the range of several hundred kelvins, in contrast to differences ranging from no difference at all up to 30 kelvin in the best case, which are considered in this thesis.

Several projects have used thermal energy to power sensors. Moser et al. [3] try to harvest energy from small differences in air temperature in a road tunnel, and look at the thermal design necessary to enable harvesting.

The only work using temperature differences both during the day and during the night is [4, 5], where the heat of the sun is used during the day to heat a phase-change material, and then, during the night, the temperature gradient occurring between the heated material and the ambient air is used to generate energy as well. In this work, the heated rock fulfills the function of a heat storage device.

2

Background

This chapter will describe the Permasense project, to provide some background about the environment of the harvesting system. It also explains the basics of the thermoelectric effect, which will be used to generate electricity.

2.1 The Permasense Project

The goal of the Permasense project [6] is to measure environmental data in high alpine areas. To achieve this, a wireless sensor network (WSN) was developed with the goal of an unattended runtime of three years. The first deployment took place in 2006/2007 at the Jungfraujoch, and three more field sites, at the Matterhorn, in the Matter valley and on the Aiguille du Midi, have been added afterwards. All data is collected in real time, and can be viewed in the internet[1].

2.1.1 Matterhorn deployment

This project has focused on sensor nodes deployed at the Matterhorn, but the general principle should be applicable for other deployments in similar conditions. The deployment at the Matterhorn is used to measure rock temperature and crack movement in a permafrost environment, with the goal of achieving a better understanding of the processes happening in permafrost regions. The deployment, visible in figure 2-1, is located approximately 3450 meters above sea level, and encounters temperatures ranging from -30 degrees Celsius in winter to up to 10 degree Celsius in summer.

It consists of 33 individual sensor nodes, which transmit data to a solar powered basis station. From the basis station, data is sent using long range Wifi to another station in the Matter valley, from where it is uploaded to the backend.

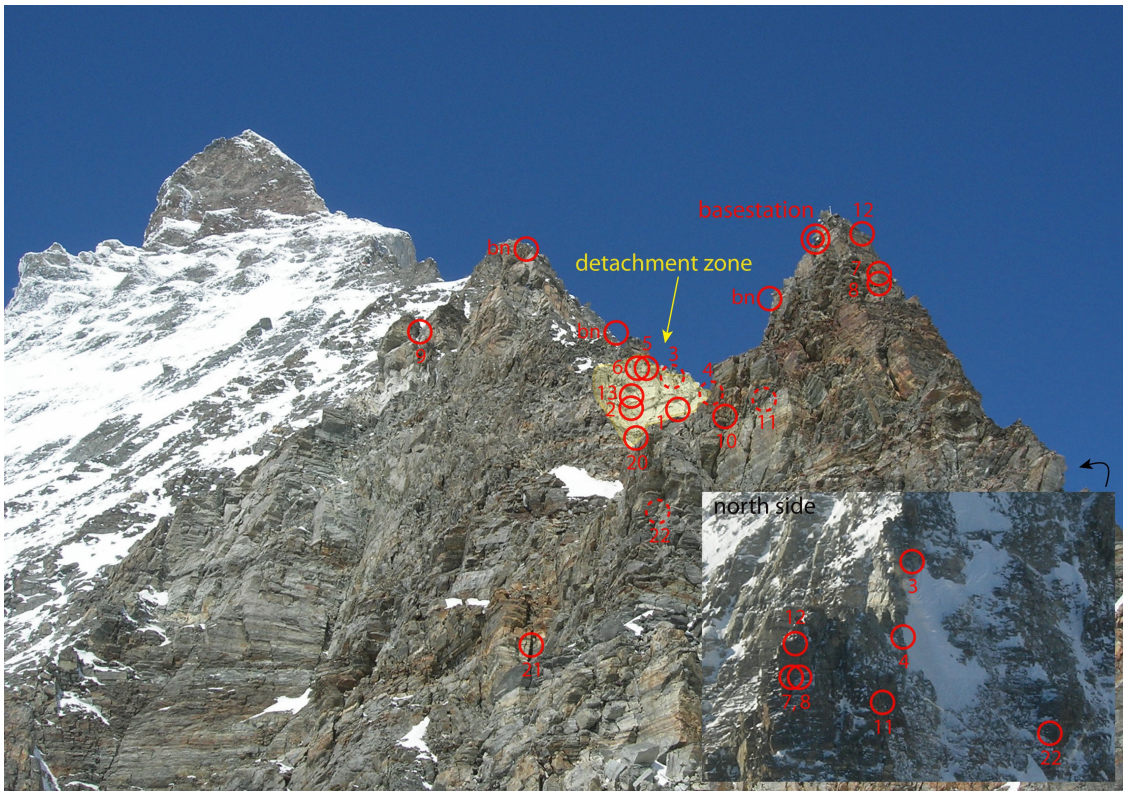

Figure 2-1
Overview of the Matterhorn deployment

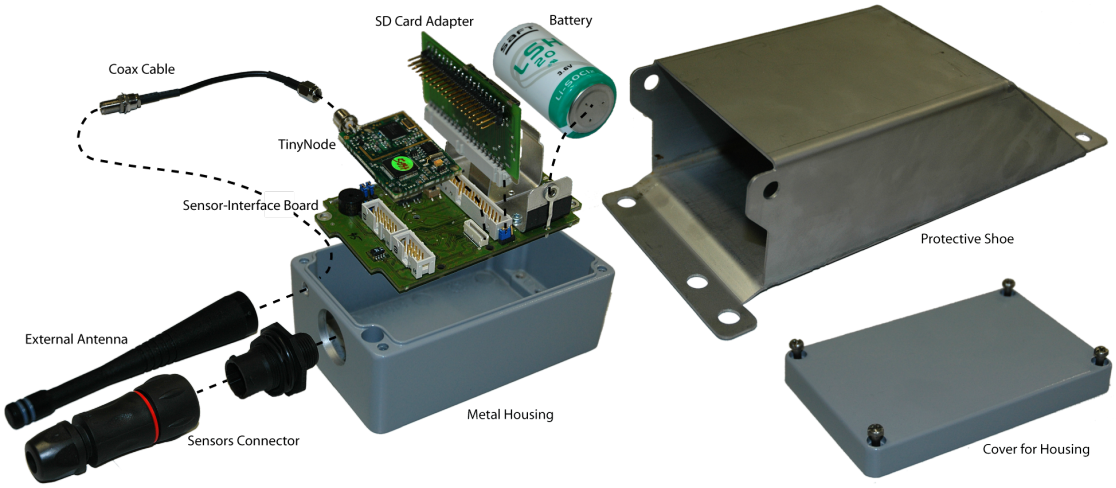

Figure 2-2
Exploded view of a sensor node

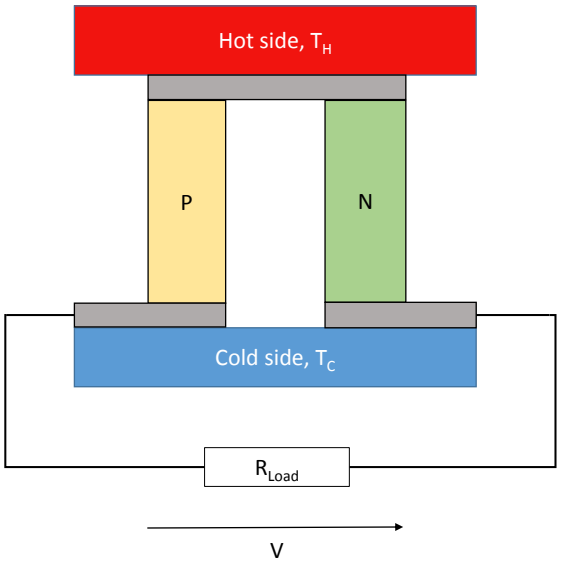

Figure 2-3
A thermocouple, consisting of a n- and p-type semiconductor

2.1.2 Sensor node

The sensor node is used as the basis of each individual sensor deployment. Figure 2-2 shows an exploded view of the components of a sensor node. The heart of the sensor node is the TinyNode (see [7]), which is mounted on the custom made sensor interface board (SIB). The TinyNode contains a microcontroller, which is responsible for reading measurements from the sensors and transmitting it to the base station by use of the integrated radio. The SIB provides interfaces for external sensors, and also contains the power supply for the node, which consists of a battery and the necessary power conversion chips. To protect the node, it is housed inside a robust, waterproof enclosure, and additionally protected from the elements by a metal casing, which is directly attached to the wall. The sensor node itself can be removed to allow easy maintenance.

2.2 Thermoelectric energy generation

There are several methods to generate electrical energy from thermal energy, but most first convert the thermal energy into mechanical energy, which is then converted to electrical energy. An example of this are the steam turbines used in nuclear power plants. As this kind of conversion is not very practical for small, remote sensors, direct conversion from thermal to electrical energy is desired.

This is achieved by use of the so called *Seebeck* effect. Discovered by Thomas Johann Seebeck in 1821, it describes the property of certain materials to produce a voltage when a temperature difference is applied [8].

Figure 2-3 shows a thermocouple, consisting of a n- and p-type semiconductor, which are connected on one end with a metal conductor. The other end is left open, and

[1] http://data.permasense.ch

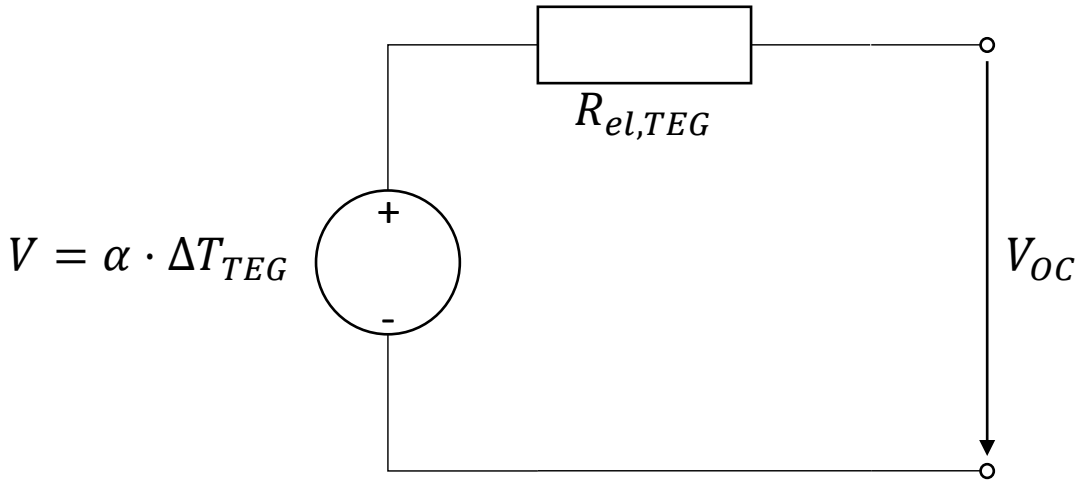

Figure 2-4
TEG modeled as temperature dependent voltage source

can be used to connect a load to the thermocouple. The resulting voltage over the load is dependent on the temperature difference $\Delta T = T_H - T_C$ between the hot and cold sides of the thermocouple. It is characterized by the Seebeck coefficient α, which describes the ratio between the generated open circuit voltage, V_{oc}, and the temperature difference ΔT.

$$\alpha = V_{oc}/\Delta T \tag{2.1}$$

Thermocouples made from a commonly used semiconductor, Bismuth Telluride, have a seebeck coefficient of only $400\,\mu\mathrm{V\,K^{-1}}$ per thermocouple, which shows that one couple alone only generates a very small voltage. Commercially available thermoelectric generators (TEGs) connect up to hundreds of these thermocouples in series, to provide a net Seebeck coefficient of the whole assembly in the range of $20\,\mathrm{mV\,K^{-1}}$ to $120\,\mathrm{mV\,K^{-1}}$.

This net generator Seebeck coefficient, together with the internal resistance $R_{el,TEG}$, allows modeling of the TEG as a temperature dependent voltage source, as seen in figure 2-4.

3

Requirements

The following section details the requirements which are posed to the energy harvesting system. They are based on the requirements for the existing sensor nodes, which are in active use. In figure 3-1, an overview of the proposed system is shown. A thermoelectric generator (TEG) is used to generate an output voltage which is then input to a DC-DC converter and power manager. From the converter, the sensor node itself is powered directly. Attached to the system is also a storage element, which can be used to store surplus energy, and bridge over times with little power generation. The following sections will detail the requirements to the system.

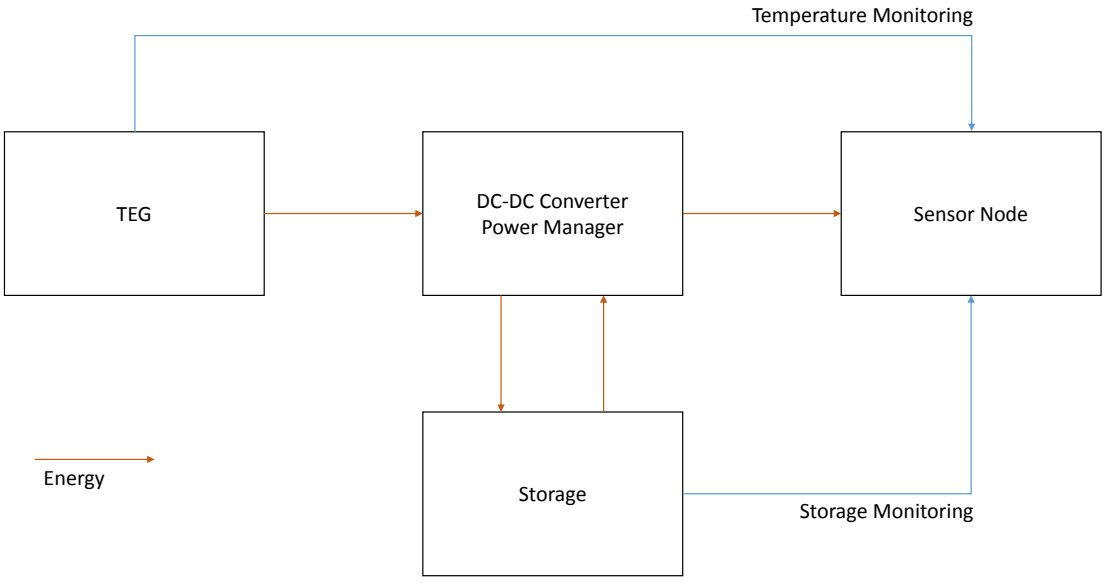

Figure 3-1
Overview of proposed system

3.1 Power generation

The main requirement of the system is the ability to harvest enough energy to power the system continuously. Based on the power requirement of the existing sensor node, this means that it has to be able to supply an average power of about $0.5\,\mathrm{mW}$ ([6]). Since the harvested energy is inherently dependent on the external conditions, it is unavoidable that there are periods where no energy can be harvested. To cover these periods, a storage element is added to the system. The requirements of the storage element will be detailed later.

3.2 System integration

As the sensor node is an existing and tested device, the harvesting system has to be attached to the node without requiring any modification at the node itself, expect for modifications in the housing required for connection of the system. This means that the harvester has to use the existing interfaces of the sensor interface board. The sensor interface board has two options for an external power supply. One option is the SDI power input, designed for a $12\,\mathrm{V}$ input, the other option is the external battery input, designed for a $3.6\,\mathrm{V}$ battery.

Any desired monitoring capabilities, such as the ability to measure voltage of the storage element or the temperature difference at the TEG, also have to implemented using existing interfaces.

3.3 Storage

The system needs some kind of energy storage, as mentioned above. The storage needs to cover two different types of power shortages. Short term energy shortages occur due to daily variations in the temperature, which lead to small periods each day where the available temperature difference is too small for power generation. There is also long-term power shortage, which can be caused by changing weather conditions and seasonal changes. Overcast sky for example leads to reduced solar irradiation, which in turn leads to a smaller temperature gradient during the day. In the worst case, a node can be covered by snow, which leads to periods lasting several weeks or even months without energy harvesting.

To allow operation even under this conditions, the storage should be able to store enough energy to allow operation for three months without any energy harvested.

3.4 Durability

The high alpine environment poses special requirements to the equipment used. The solution has to work at temperatures as low as $-30\,^{\circ}\mathrm{C}$, and be robust enough to survive rockfall and moisture.

3.5 Feasability

The energy harvesting system has to be integrated into the existing system, which is in active use. It is installed in a high alpine region, which means that access is diffi-

cult and limited. Because of this, special care also has to be taken to make sure that installation is as easy as possible. This means that a feature like the buzzer, which is used in the existing sensor node to indicate successful system startup, has to be preserved. The size and effort of any installations, like drilling boreholes, should also be kept to a minimum. The size of a borehole for example, should be limited to at most $20\,\mathrm{cm}$, and it should not be wider than $20\,\mathrm{mm}$. This has to be considered during the design of the system.

4

Power Source Characterisation

The following section provides a characterization of the temperature gradients at the Matterhorn. It details average and maximum differences, which can be expected, compares different positions, and describes the typical temperature profile of a day, as well as the seasonal changes in temperature.

4.1 Basic Principle

The idea of a thermal energy scavenging system is to use a naturally occurring thermal gradient to harvest energy. In the permafrost environment, these gradients occur due to the high thermal capacity of the rock. During the day, the rock surface gets heated up, due to both direct solar irradiation as well as through the warmed up ambient air. During the night, the rock cools down again. Because of the high thermal capacity of rock, only the surface area follows this temperature change, while deeper sections experience are much slower to respond. Figure 4-1 shows temperature measurements from different locations, demonstrating the differences between the surface measurements and measurements taken deeper inside the rock.

4.2 Sensors

This section will describe the sensors at the Matterhorn, from which the temperature measurements used for the characterization are taken. All data is also available online[1]. To analyze the available thermal gradients, measurement from both the surface, as well as from the inside of the rock are necessary. Fortunately, there are sensors which provide this data. For surface data, several measurements can be used. A temperature sensor is included inside each sensor node, and thermocouples are placed directly on the rock surface. In addition to this, each crackmeter also includes a temperature sensor. Measurements from inside the rock are provided by two types of sensors, sensor rods and thermistor chains. The sensor rod is one meter long, and contains four temperature sensors, allowing measurement

[1] http://data.permasense.ch

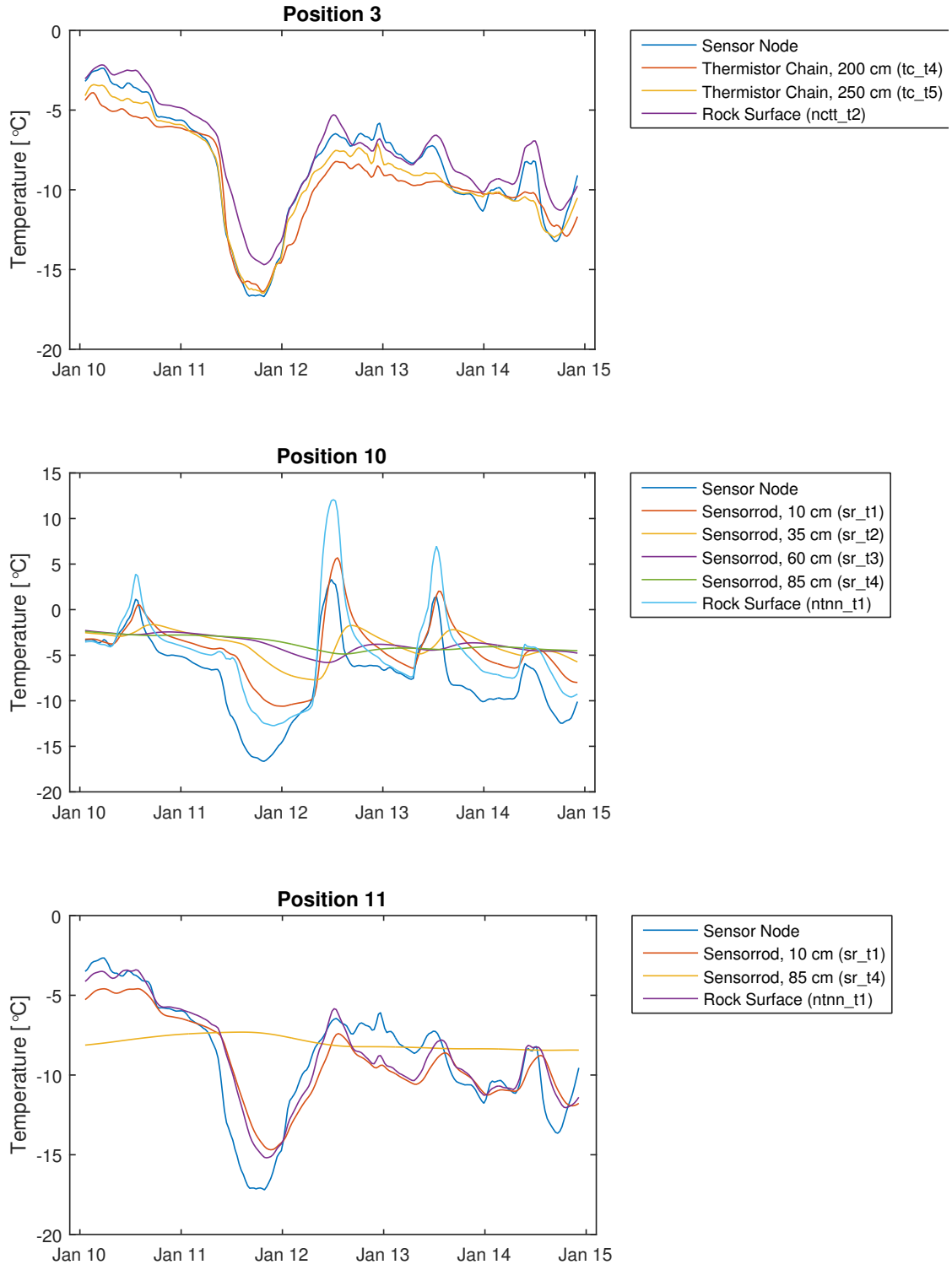

Figure 4-1
Temperature measurements from the Matterhorn deployment

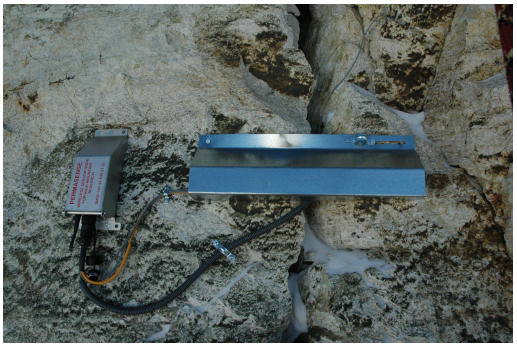

Figure 4-2
Sensornode with attached crack meter (below shielding) and thermistor chain (black cable)

Figure 4-3
Crackmeter

at different depths. It is placed in a borehole which is drilled perpendicular to the rock surface. The thermistor chain consists of 5 thermistors on a cable, with $50\,\mathrm{cm}$ of space between them. It is placed inside a crack or a bore hole. Figure 4-2 shows a thermistorchain deployment, while figure 4-3 depicts a crackmeter.

4.3 Bipolarity

An important characteristic of this power source is the reversal of the temperature gradient during the night, which is unlike most applications of thermal energy harvesting, where a constant temperature gradient is assumed. As seen in figure 4-1, the temperature gradient usually changes polarity twice a day, once in the morning, when the surface gets heated up and becomes warmer than the inside, and once in the evening, when the surface cools down again. But, as is also visible, this sometimes does not happen, depending on the weather conditions.

4.4 Position influence

As already mentioned earlier, the temperature gradient is dependent on the position of the sensor node. Position 10 is facing south, and the plot shows the surface temperature rapidly rising, as soon as the solar irradiation starts to warm up the rock. Depending on the weather conditions, the amount of this warming also changes significantly. On 11 January, there is even no warming at all, on the contrary, the temperature drops about 10 degrees. The other two positions are facing north, and the temperatures reach less extreme values, especially during the day.

Table 4-1 shows average and maximum temperature gradients which occurred between the years 2011 to 2014. Position 10 clearly has the highest average gradient, with both the other positions having smaller gradients. This shows that the solar irradiation plays a significant role in creating a temperature gradient, but also that even without direct solar irradiation, temperature gradients of more than $20\,\mathrm{K}$ occur.

Position	sensor	average ΔT	max ΔT pos.	max ΔT neg.
3	tc5	2.23	20.48	-11.52
10	sr_t4	5.29	22.95	-21.08
11	sr_t4	3.70	25.27	-16.00

Table 4-1: Temperature difference statistics for positions 3, 10, and 11, with Sensor Node temperature taken as surface measurement. Years 2011–2014.

Figure 4-4
Temperature measurements inside sensor node

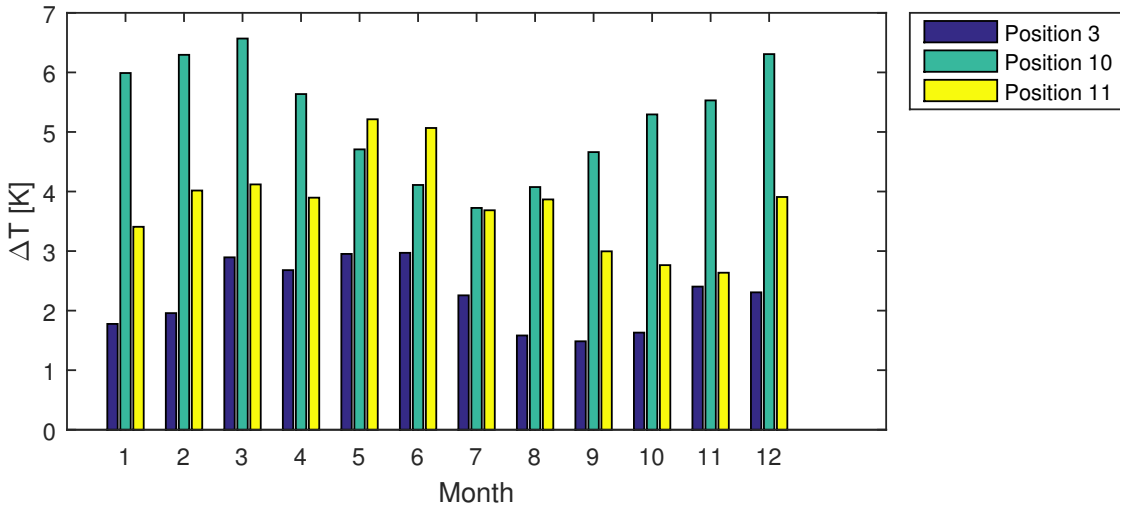

Figure 4-5
Average temperature difference per month

4.5 Seasonal variations

In addition to short term changes occurring due to weather effects, the temperatures also undergo seasonal changes. Figure 4-4 shows the temperatures inside the sensor nodes. While these temperature changes do not effect the thermal harvesting directly, they are important factors in designing the system. They define what kind of temperatures the system has to endure, and have to be taken in account when selecting components.

Not only the absolute temperature changes depending on the season, also the gradients do. During the year, both the intensity and angle of solar irradiation change, which leads to a seasonal pattern in the temperature differences, which is shown in figure 4-5. Interesting to note here are the variations between the positions. Position 10 experiences the most variation, and also shows bigger gradients during the winter months, although it would be expected that a south facing position would have bigger gradients during the summer, when solar irradiation is most intense. A possible explanation for this can be found in the near environment of the sensor node. Just below the node are several ledges, which are covered with snow during winter. Reflections from these ledges could increase the solar irradiation at the node position, and lead to bigger gradients. The other positions show a more traditional pattern, where the early summer months of May and June exhibit the largest gradients.

5

Modelling

To evaluate the feasibility of energy harvesting, the system was modeled in Matlab. The following chapter will explain this model.

5.1 Temperature data

Thanks to the existing deployments, temperature data from several positions and over several year is available. Using a Matlab script, the temperature data is downloaded from the Permasense backbone. As the measurements come from different sensors, they then have to be normalized. This is achieved by downloading the data in the original resolution, and then resampling all sensor data with the same time vector. As the temperature changes slowly, this does not lead to a loss of information.

5.2 Temperature gradient

Figure 5-1 shows a sketch of the proposed harvesting system. Using a borehole, a thermal guide is inserted into the rock. The thermal guide consists of a good thermal conductor, which is attached to the TEG on one end, and to the rock at the other

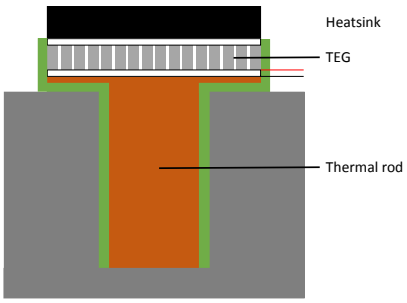

Figure 5-1
Sketch of the thermal rod design

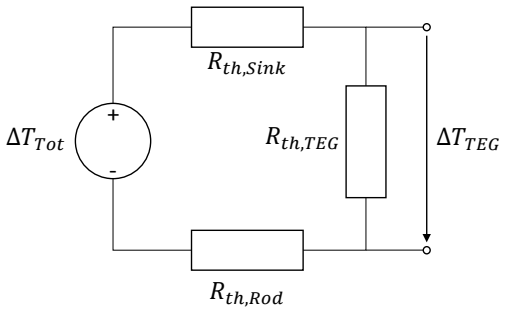

Figure 5-2
Schematic of thermal system

end. The walls are insulated, to make sure that no heat is lost to the rock, and the maximum gradient is formed over the TEG On the other side of the TEG, a heatsink is attached, which is exposed to ambient air. During this work, the temperature inside a sensor node is assumed to be equal to the temperature of the heatsink in the proposed system.

Based on the temperature data, the actual temperature gradient over the TEG can be modeled. For this, the thermal resistances of all elements have to be taken into account. Figure 5-2 shows the resulting system. The resistances of the connections between the different system parts are included in $R_{th,Rod}$ and $R_{th,Sink}$. Similar to an electric circuit, the temperature drop ΔT_{TEG} can now be calculated from the total temperature difference ΔT_{Tot} as follows:

$$\Delta T_{TEG} = \Delta T_{Tot} \frac{R_{th,TEG}}{R_{th,TEG} + R_{th,Sink} + R_{th,Rod}} \tag{5.1}$$

Based on this schematic, a maximum thermal resistance $R_{th,TEG}$ seems to provide the biggest temperature drop over the TEG. But to maximize the power output, not only the temperature difference, but also the heat flow has to be considered, as this influences the available current. Making $R_{th,TEG}$ as high as possible limits the heat flow, and is thus not optimal. In [9] is is shown that the assumption of a matched load resistance, $R_{th,TEG} = R_{th,Rod} + R_{th,Sink}$, can be used to estimate the temperature drop over the TEG itself for the case with maximal power output. Combining this with equation (5.1), this leads to the following simple calculation:

$$\Delta T_{TEG} = \frac{1}{2} \Delta T_{Tot} \tag{5.2}$$

5.3 Power generation

Based on this equation, we can now calculate the power output of the TEG for a given temperature difference. With the help of the Seebeck coefficient α, introduced in section 2.2, the open circuit voltage U_{oc} can be calculated.

$$U_{oc} = \alpha \cdot \Delta T_{TEG} \tag{5.3}$$

Together with the internal electrical resistance of the TEG, $R_{el,TEG}$, we can now calculate the power which can be harvested with a given TEG.

$$P = U_{load} \cdot I = \frac{U_{load}^2}{R_{load}} = U_{oc}^2 \cdot \frac{R_{load}}{(R_{load} + R_{TEG})^2} \tag{5.4}$$

For maximum power transfer, the load resistance R_{load} has to be equal to R_{TEG}. This means that the maximum power generated can be calculated as follows:

$$P_{max} = \frac{1}{4} \cdot \frac{U_{oc}^2}{R_{TEG}} = \frac{1}{4} \frac{\alpha^2}{R_{TEG}} \cdot \Delta T_{TEG}^2 = \frac{1}{16} \frac{\alpha^2}{R_{TEG}} \cdot \Delta T_{Tot}^2 \tag{5.5}$$

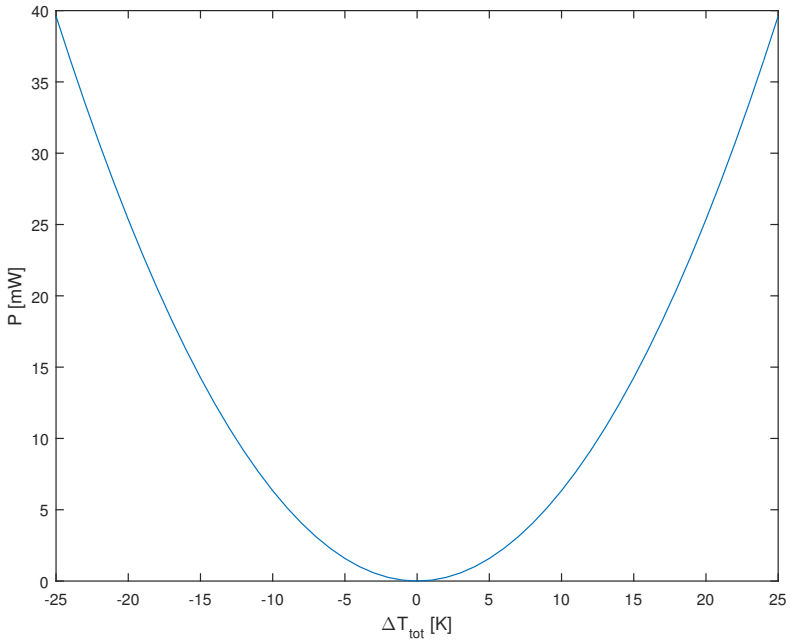

Figure 5-3
Maximum power output for total temperature gradient, calculated based on the TEG 127-175-25

	η_{conv}	$V_{startup}$	$V_{harvest}$
LTC3109	0.3	$\pm 30\,\mathrm{mV}$	$\pm 30\,\mathrm{mV}$
bq25504	0.6	$330\,\mathrm{mV}$	$130\,\mathrm{mV}$

Table 5-1: Converter parameters for model

For an initial evaluation, the TEG 127-175-25 from Thermalforce was chosen, with Seebeck coefficient $\alpha = 60\,\mathrm{mV\,K^{-1}}$ and resistance $R_{TEG} = 3.55\,\Omega$. The TEG has a size of $30\,\mathrm{mm}$x$30\,\mathrm{mm}$. Figure 5.3 shows the maximum power output over the range of temperature gradient which can be encountered at the Matterhorn.

With this TEG, a ΔT_{tot} of $\pm 2.8\,\mathrm{K}$ is needed to generate the $0.5\,\mathrm{mW}$ needed by the sensor node. Compared with the average values from table 4-1, this shows that with this TEG, reaching the power required for the sensor node seems achievable for positions 10 and 11, while the average difference at position 3 seems to low. But, as is visible from the figure, the power generation rises quadratically with the temperature difference, which means that the missing energy could be harvested in times with higher gradients, and then stored.

5.4 Conversion

One of the key elements for a system harvesting energy from small temperature differences is a DC-DC converter which converts the input voltage, which is in the range of ten to several hundreds millivolts, into a suitable voltage for storage and use by the sensor node. The number of ready made converters on the market which

specialize in conversion of small voltages is very limited, only two offerings were found. The BQ25504 [10], produced by Texas Instruments, and the LTC3109 [11] by Linear Technology.

The bq25504 is a DC-DC converter capable of working from input voltages as low as $80\,\mathrm{mV}$. It features an integrated battery management system, which allows configuration of a lower and upper battery threshold voltage. The battery voltage is also used to power the attached system. It features a configurable power good output signal.

The LTC3109 allows startup from an even lower voltage of $30\,\mathrm{mV}$, and is able to work with bipolar voltage sources. It can use one storage element, which it will charge to a voltage of $5.25\,\mathrm{V}$. There are two regulated outputs, one of which can be switched on and off by the attached system. The voltage of these outputs is configurable by the user.

Based on the factors mentioned above and further datasheet information, each converter was modeled with a conversion efficiency η_{conv}, a startup voltage $V_{startup}$, and a harvesting voltage $V_{harvest}$. In addition, the LTC3109 has the ability to harvest from bipolar voltages, while the bq25504 is limited to one polar ity only. To simulate this, the absolute value of the input voltage was considered for bipolar case, and only the positive part for the unipolar case. Table 5-1 shows the parameters used for the model. Based on this, the power available to the SIB and storage element can be calculated.

5.5 Storage

The remaining element in the model is storage. Two factors are relevant for the model. First, the size of the storage, and second, the ability of the storage to retain charge. In contrary to modeling the power output, this cannot be modeled time independent.

The size of the storage is straightforward to model, but the usable voltage has to be taken into account. Due to the design of the converters, the storage can only be used down to a certain voltage, which is the output voltage for both converters. More important for the system is modeling the leakage current of the storage element. Each storage technology has some kind of leakage, which plays a significant part in designing a system running for long periods. The details of the leakage current depend on the storage technology used. For the model it was assumed that the energy would be stored in a capacitor, and that the leakage current would is constant in time, not dependent on the voltage.

5.6 Sensor board power

To evaluate the performance of the system, the sensor node itself also has to be modeled. There are two cases to be considered, system startup and normal system operation. As the system will spend most time in operation, and ideally only starts up once, only the power consumption of the running system is used in the model. Figure 5-4 shows a measurement of the current consumed by the sensor node during

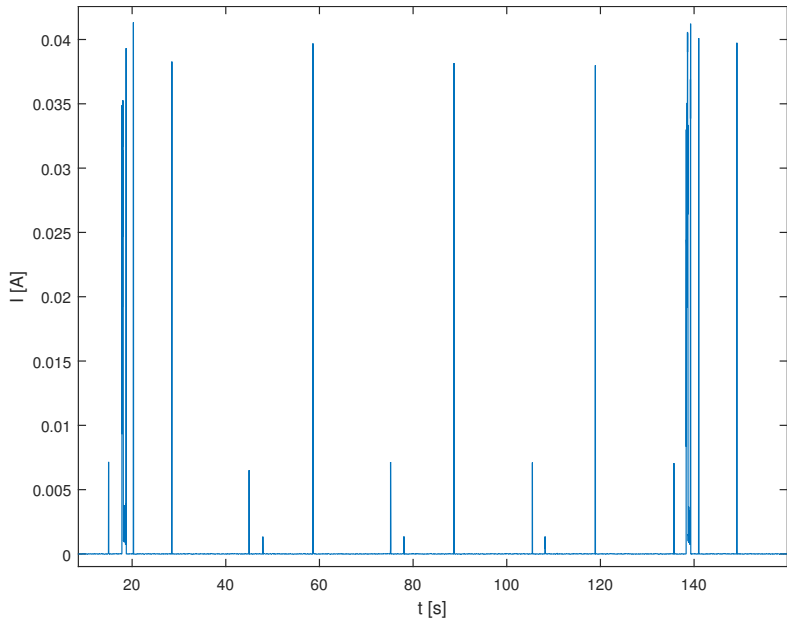

Figure 5-4
Current measurement of the Sensor node

position	sensor	converter	energy harvested [%]	uptime [%]
3	tc_t5	LTC3109	35	8
3	tc_t5	bq25504	14	7
10	sr_t4	LTC3109	156	61
10	sr_t4	bq25504	88	40
11	sr_t4	LTC3109	85	26
11	sr_t4	bq25504	44	16

Table 5-2: Results of initial model evaluation, with surface temperature taken from inside the sensor node. TEG used: TEG 127-200-25 from Thermalforce

operation. It is visible that most of the time, the system is in a very low power mode, and it wakes up periodically to perform measurements, and send and receive data. On average, the power requirement of the node is $0.5\,\mathrm{mW}$, and this is used in the model. System startup will be discussed later, in the context of the prototype.

5.7 Model evaluation

The following sections will discuss results obtained from this initial model, namely the questions whether harvesting is possible with only a shallow borehole, if bipolar harvesting is more effective than unipolar harvesting, and the influence of the storage element on the achievable runtime.

sensor	depth [cm]	energy harvested [%]	uptime [%]
sr_t1	10	89	28
sr_t2	35	158	60
sr_t3	60	160	62
sr_t4	85	156	60

Table 5-3: Harvested energy and uptime for different depths, with converter LTC3109 and TEG 127-175-25

5.7.1 Bipolarity

In the Matterhorn environment, the polarity of the gradient changes. This enables the system to harvest both during the day and during the night, but at a cost. The ability of the converter to harvest from bipolar voltages also has an influence on the conversion efficiency. For the converters mentioned above, this means that the bipolar harvester only has 50 percent of the efficiency of the unipolar harvester. This leads to the question whether bipolar harvesting is worth the loss in efficiency. To answer this, the power generated by both the unipolar and the bipolar harvester was estimated, based on temperature data between the years 2011 and 2014. Table 5-2 shows the result. The energy harvested is given as percentage of the total energy needed to sustain a power requirement of $0.5\,\mathrm{mW}$. The uptime is calculated based on the percentage of total time, where enough energy is available to supply the sensor node with power. The cost of system startup is not considered. Based on these results, the bipolar converter clearly seems to have the lead. To enable comparison between the different values, the sr_t4 measurement was used for both position 10 and 11, although a real system would have to use a less deep borehole, as will be discussed in the next section.

5.7.2 Thermal rod depth

One of the questions with the setup in this project is the depth of the thermal guide which is necessary for the harvesting unit to generate enough power. Different depths experience different temperatures, which means that the efficiency of the harvester depends on the depth of the thermal rod. The sensor rods used at the Matterhorn allow a comparison between different depths. This analysis is concentrated on position 10, because it has the best data quality. The sensor rod has four thermistors at depths of 10, 35, 60 and 85 cm. Table 5-3 shows the modeled performance for these depths. The first measurement, from a depth of $10\,\mathrm{cm}$, shows a significantly worse performance than the other depths. The requirement for the borehole (see section 3.5) states that the depth should be at most $20\,\mathrm{cm}$. There is no measurement at this exact depth, but it can be assumed that the performance would be somewhere between the performance of the sr_t1 and sr_t2 measurements. As the performane increases with the depth of the borehole, the maximum feasible depth of $20\,\mathrm{cm}$ is recommended.

5.7.3 Storage size

Another issue is the size of the storage element. If leakage wasn't an issue, the storage element could just be as big as possible. But unfortunately, the leakage current of supercapacitors increases with the capacity.

This means that bigger capacitors can actually decrease the system efficiency, as the high leakage current means that the stored energy is mostly wasted. On the other hand, when the capacitors are too small this means that potentially useful energy is wasted.

For the initial requirement of 3 months of energy harvesting, the storage element would need to store at least $3900\,\mathrm{J}$, not considering leakage and based on a power requirement of $0.5\,\mathrm{mW}$. Based on an usable voltage range from $5.25\,\mathrm{V}$ to $3\,\mathrm{V}$, this leads to a minimum capacitance of $420\,\mathrm{F}$. A storage element consisting of 5 capacitors with size $90\,\mathrm{F}$ each, which would fulfill this requirement, has a leakage current of about $2.5\,\mathrm{mA}$, which is an order of magnitude bigger than the current consumed by the sensor node, which is only $148\,\mu\mathrm{A}$ (see [6]). In addition, this leakage current limits the maximum reachable backup time to about 4.5 days, as the capacitors will have discharged themselves in that time. Clearly, a backup time of 3 months cannot be reached by a solution only using supercapacitors.

Ignoring any long time backup requirement, the question is which size of super capacitor offers the best tradeoff between leakage and capacity. To analyze, the system was simulated over several years with different capacities. An upper bound for the achievable uptime is given by the amount of energy harvested, as shown in table 5-2. The estimated uptime achieved with two supercapacitors of size $15\,\mathrm{F}$ shows that more than fifty percent of the energy is harvested in vain, as it cannot be used by the system.

Figure 5-5 shows that with increased storage, which also means increased leakage, the achievable system uptime decreases. This indicates that leakage is the deciding factor when choosing a storage element.

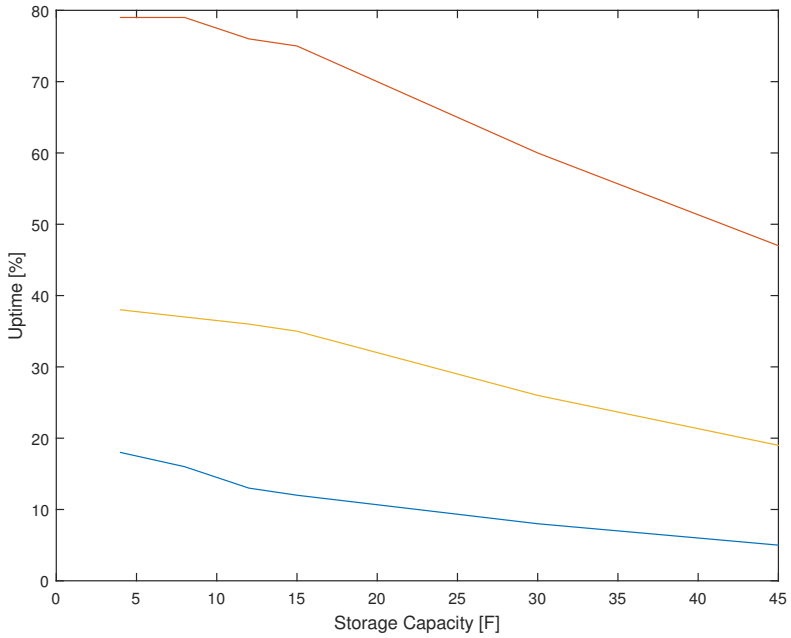

Figure 5-5
Evaluation of the effect of storage size on system uptime

6

Electrical Prototype

This chapter will discuss the prototype system, which was used to test the electrical part of the system, from the TEG at one end to the SIB at the other end. Figure 6 shows an picture of the prototype circuit board, to which the TEG and the SIB are attached.

6.1 Overview

The TEG is connected to the input of the bipolar DC-DC converter, which converts the small input voltage to an output voltage of $3.3\,\mathrm{V}$. In the case when there is more power available than currently needed by the sensor node, the storage element is used to store it. Similarly, if the TEG does not provide enough energy, the storage element is used to cover the gap. The external battery input of the sensor node is connected to the output of the converter. In addition, the storage voltage is attached to the SDI voltage input, to allow monitoring of the storage voltage. The following sections will detail the individual parts of the system.

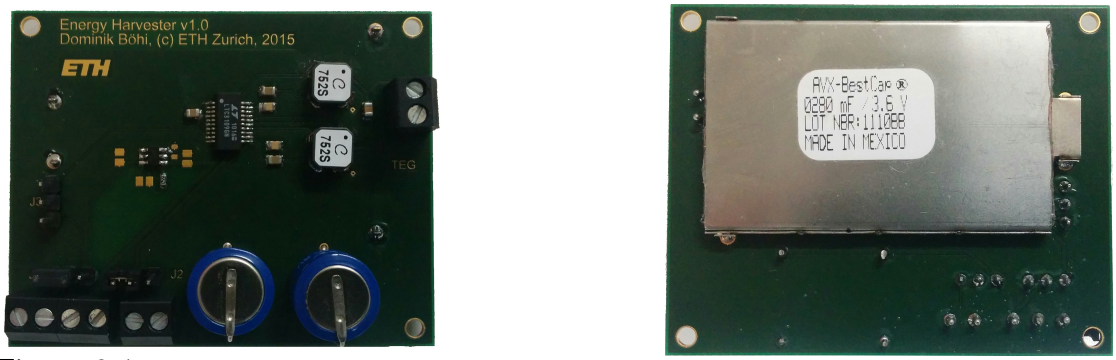

Figure 6-1
Printed circuit board containing the DC-DC converter and the storage capacitors.

6.2 Converter

For the prototype system, the LTC3109 was chosen, based on the evaluation in section 5.7.1. This converter allows bipolar harvesting, and can start from voltages as low as $\pm 30\,\mathrm{mV}$. The configurable output voltage is set to $3.3\,\mathrm{V}$, which can be used by the external battery input of the SIB. The power good output is used by the optional load switch, which is detailed later.

6.2.1 Output stabilization

The current from the storage element to the converter output is limited, which means that the current for a pulse load has to be supplied by a capacitor at the output. The biggest pulse load in this system occurs during startup. The buzzer, which is used to indicate system startup, draws an average current of $28.8\,\mathrm{mA}$, over a period of 2 seconds. This is an important feature during deployment to verify that the sensor node is working. As deployment often has to be done by using rope access, it is essential that correct operation of the system can be easily verified. The necessary output capacitance can be estimated by the following formula, taken from the datasheet:

$$C_{out} \geq \frac{I_{pulse} \cdot t_{pulse}}{\Delta V} \tag{6.1}$$

With an allowed voltage drop of $0.3\,\mathrm{V}$, based on the minimum input voltage of $3\,\mathrm{V}$ of the SIB, the required capacitance is:

$$C_{out} \geq \frac{28.8\,\mathrm{mA} \cdot 2\,\mathrm{s}}{0.3\,\mathrm{V}} = 283\,\mathrm{mF} \tag{6.2}$$

This capacitance is big enough that one needs to use a specialized capacitor. The BestCap series from AVX [12] is designed for pulse loads, and a $560\,\mathrm{mF}$ capacitor was chosen for the output. During operation, the output capacitor has to supply the current required when then system wakes up. Figure 5-4 showed these pulses, based on the length and current consumption of these pulses it can be shown that the $280\,\mathrm{mF}$ capacitor is also sufficient.

6.2.2 Output disconnect

The large current needed at startup also makes it necessary to have some kind of load disconnect during startup. When the system is starting up again after a period of no power, the sensor node will start before the necessary startup voltage is reached. This leads to a voltage drop which leaves the sensor node in an inconsistent state, where it consume more power than usual, and which prohibits a normal startup.

To avoid this, a load disconnect is integrated in the prototype. The voltage good signal available is used to only connect the sensor node when the voltage level at the output is within nine percent of the programmed $3.3\,\mathrm{V}$. To allow testing of the load disconnect feature, a jumper allows switching between operation with and without load disconnect.

6.3 Storage

As mentioned in the requirements, the goal was to achieve a runtime without energy harvesting of three months. In section 5.5 we found that using supercapacitors, this goal cannot be reached. For the prototype system, other technologies were also evaluated. The following sections give a short overview.

6.3.1 Lithium-Ion capacitors

A new technology, called Lithium-Ion supercapacitor, offers a promising alternative to conventional supercapacitors. They offer similar capacities, but have far smaller leakage currents [13]. But due to the Lithium-Ion technology used, they also have more limits in their usage, having a minimum discharge voltage as well. They are also fairly expensive, costing about 50 CHF for a $270\,\mathrm{F}$ capacitor.

6.3.2 Rechargeable battery

Another option would be the use of a conventional rechargeable battery, such as a Lithium-Ion or Nickel-Cadmium based accumulator. These are offered with huge capacities, and with excellent ability to retain their charge over a long time. But, due to their design, they require a battery management system, which makes sure that they are properly charged and discharged. The ability to charge them at low temperatures is also limited, with most technologies only allowing charging at temperatures from zero degrees upwards.

6.3.3 Supercapacitor

For the prototype, normal super capacitors were chosen as storage, despite their limitations. Conventional accumulators are not usable to the impossibility to charge them at low temperatures, and the requirement of a battery management system, which is not present in the selected converter, and would waste too much energy when implemented externally. The Li-Ion capacitors seem like an ideal solution, but are only offered with maximum voltage ratings of $3.8\,\mathrm{V}$, which is not directly compatible with the $5.25\,\mathrm{V}$ storage output of the converter. Using two capacitors in series would solve this limitation, but leads to the issue of balancing. It also means that the effective capacity would be halved, making this already expensive solution even more so. Considering this, normal super capacitors were chosen, even thought this means that the requirement of 3 months of independent operation cannot be reached.

6.4 System integration

The prototype needs to be connected to the sensor node. To achieve this, it uses the external battery input of the SIB. This input is designed for a $3.6\,\mathrm{V}$ battery. The input voltage is then converted by a low dropout linear regulator to a voltage of $2.8\,\mathrm{V}$, to supply the TinyNode. In addition, several other voltage regulators are used to power other subsystems. These regulators are switchable and managed by the TinyNode. This solution is clearly not optimal, as the voltage regulated output

of the harvesting chip is directly input to another voltage regulator. Due to the requirement that the harvesting system has to be integrated into the existing sensor node, this is unavoidable. An advantage of the external battery input is the presence of voltage monitoring, which means that the output voltage of the harvesting system can be easly monitored by the sensor node. To achieve monitoring of the storage capacitor, the storage voltage is connected to the SDI power input. The SDI input can be switched off, which then allows use of the SDI input voltage capability to measure the storage voltage. This achieves monitoring of the storage voltage without using an ADC channel, which then can be used for an external sensor.

7

Evaluation

This part will describe the evaluation of the prototype, and offer a comparison with the model. First, the general harvesting efficiency of the system is discussed. Then, the special case of system startup will be evaluated. Finally, the ability of the system to provide power during periods without energy harvesting is analyzed.

7.1 Efficiency

The efficiency of the prototype was evaluated by measuring the harvested energy for different TEGs at a range of different temperatures. As the integrated storage of the prototype is quite large, a small external capacitor was used to measure the efficiency.

7.1.1 TEG selection

The choice of thermo electrical generator has to take into account both the converter used as well as the constraints due to location. Only a small amount of manufacturers produce thermoelectric modules especially designed for energy generation, most are intended to be used to as heater or cooler. Due to the small market size, the datasheets available for TEGs vary greatly in the amount of detail they provide, and usually the data is only given for applications with temperature differences in the range of $200\,\mathrm{K}$. This makes it necessary to measure the TEGs directly to evaluate the necessary parameters for a simulation. The Seebeck coefficient has to be

Name	$\alpha\,[\mathrm{mV\,K^{-1}}]$	$R_{el}\,[\Omega]$	$R_{th}\,[\mathrm{K\,W^{-1}}]$
TEG 127-175-25	60	3.6	3.7
TEG 241-150-29	96	10.0	2.3
TEG 127-200-28	56	6.6	5.6
GM200-71-14-16	28	2.1	-

Table 7-1: List of evaluated TEGs

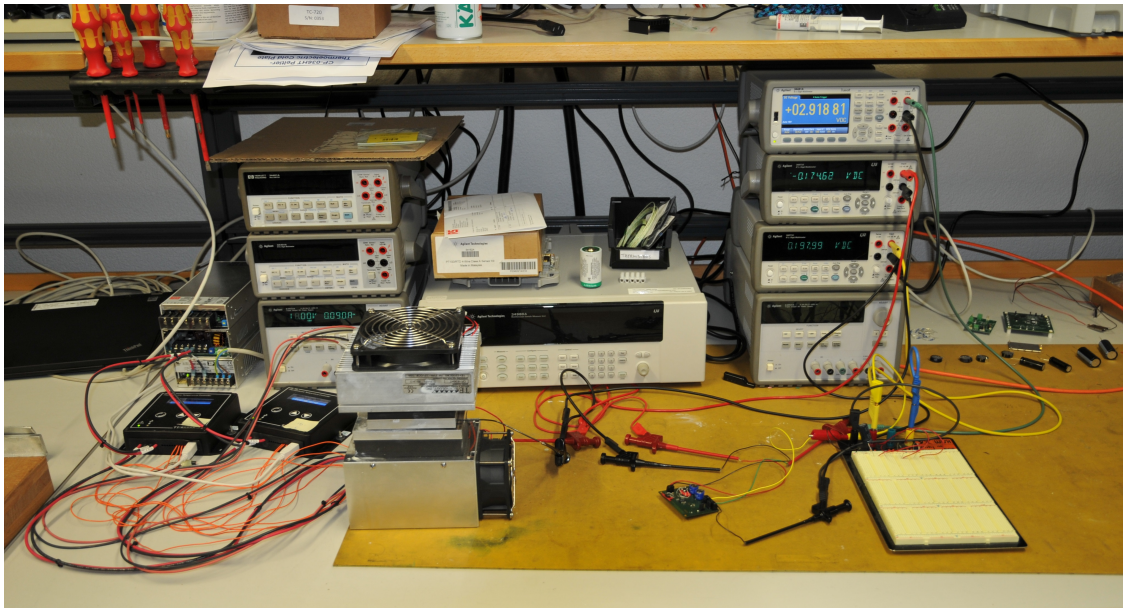

Figure 7-1
Test setup used to measure prototype efficiency.

defined, and the combination of TEG and converter has to be evaluated. To limit the amount of TEGs to be tested, a choice was made based on equation 5.5, which shows that the maximum power for a given ΔT is proportional to the ratio $\frac{\alpha^2}{R_{TEG}}$, which are both parameters of the TEG. For a range of resistances covering the optimal input resistance range of $2\,\Omega$ to $10\,\Omega$ of the converter, the TEGs with the highest Seebeck coefficient where chosen for evaluation. Table 7-1 shows the parameters of the evaluated TEGs, either taken directly from the datasheets, or calculated based on them [14–17].

7.1.2 Measurement setup

Figure 7-1 shows a picture of the test setup used. On the left hand side are two cold plate coolers which are used to control the temperature difference over the TEG.The thermal controllers of the coolers allow setting the exact temperature at both sides of the TEG. In the middle, the prototype board is connected to the TEG and the external storage, visible on the breadboard to the right. The digital multimeters in the background are used to monitor the TEG voltage and the storage voltage.

To measure harvested energy, a $3300\,\mu F$ capacitor was attached to the external storage connection of the prototype. Starting from a fully charged output cap and a discharged storage cap, the time it took the harvester to charge the storage capacitor to a voltage of $5.15\,V$ was measured. This voltage was determined to be the maximum voltage to which a capacitor is charged by the DC-DC converter. It is within specification of the converter, nominal voltage would be $5.25\,V$.

Figures 7-2 and 7-3 show the result of the measurement. The efficiency is calculated based on the maximum possible power output, calculated using equation 5.5. Based on these measurements, the TEG 127-175-25 from Thermalforce offers the best per-

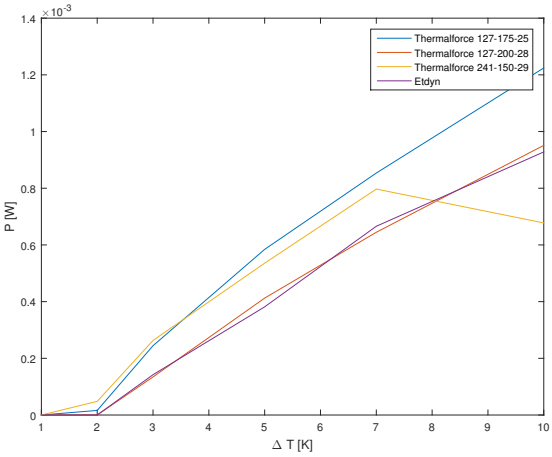

Figure 7-2
Harvested power for different TEGs

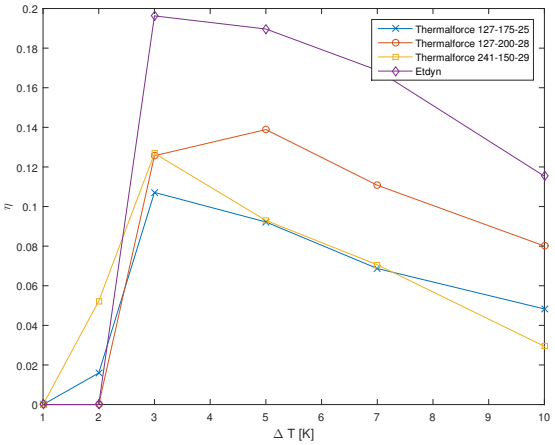

Figure 7-3
Efficiency of the energy harvesting system

formance. Although it isn't the best in regards to efficiency, it still offers the best overall performance. The results also indicate that the efficiency of the converter is dependent on both the used TEG as well as on the temperature difference.

Based on these results, it is not feasible to use bipolar power harvesting. The low efficiency of the DC-DC converter negates the additional energy which can be harvested during the night.

7.2 Startup

Another issue is system startup after a period of no power. The SIB is designed with battery power in mind, which means that the system only has to start when a new battery is inserted. This means that the startup sequence is not designed for low power, but to provide immediate feedback whether the system has successfully started. As the nodes are deployed at hard to reach locations, this is necessary to ensure efficient deployment. Confirmation of system startup is done with a buzzer, which is sounded twice.

To test system startup, the output capacitor was completely drained, and storage was disconnected. For a first test, the sensor node was directly attached to the converter output, with no switch in-between. The measured voltages are shown in figure 7-4. This resulted in the system being caught in an unstable operating condition, where the output voltage reaches $1.6\,\mathrm{V}$, and then the sensor node starts up and discharges the output, until the sensor node shuts down again. The system stays in this loop for several minutes, until it reaches a stable condition, where the output can charge up to $3.3\,\mathrm{V}$. The sensor node is then in a kind of brown out state, where it draws a continuous current of $30\,\mathrm{mA}$, but is not started correctly. This leads to the system being unusable.

To avoid this problem, an output switch was integrated into the prototype, to switch off the output voltage while the capacitors are charging. The power good output of the LTC3109, which goes high when the output voltage reaches regulation, is used to switch the voltage. Figure 7-5 shows the resulting voltage measurements. The load

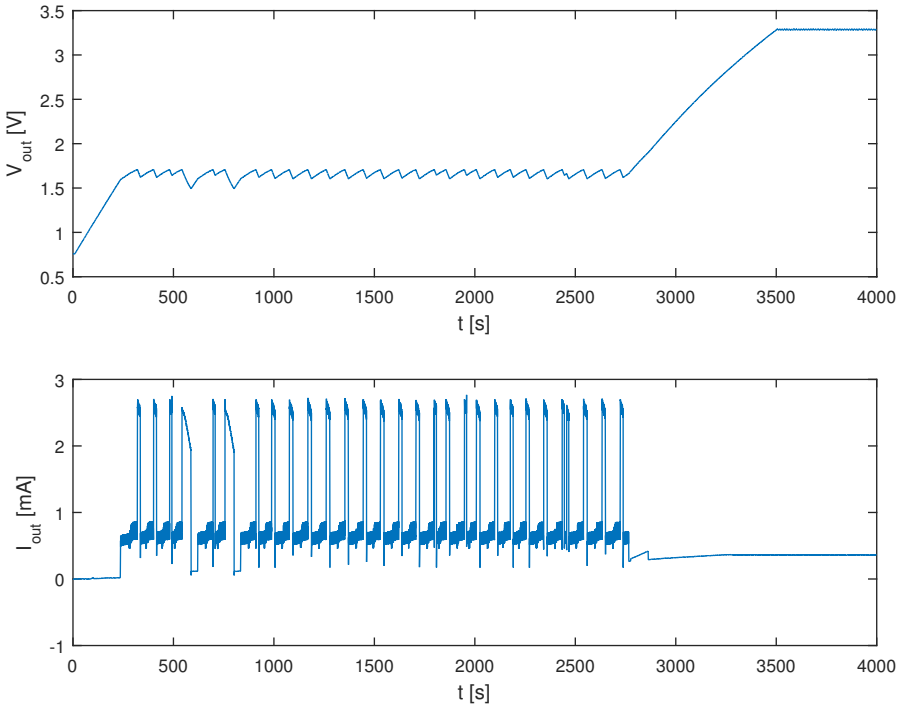

Figure 7-4
Startup with directly connected output

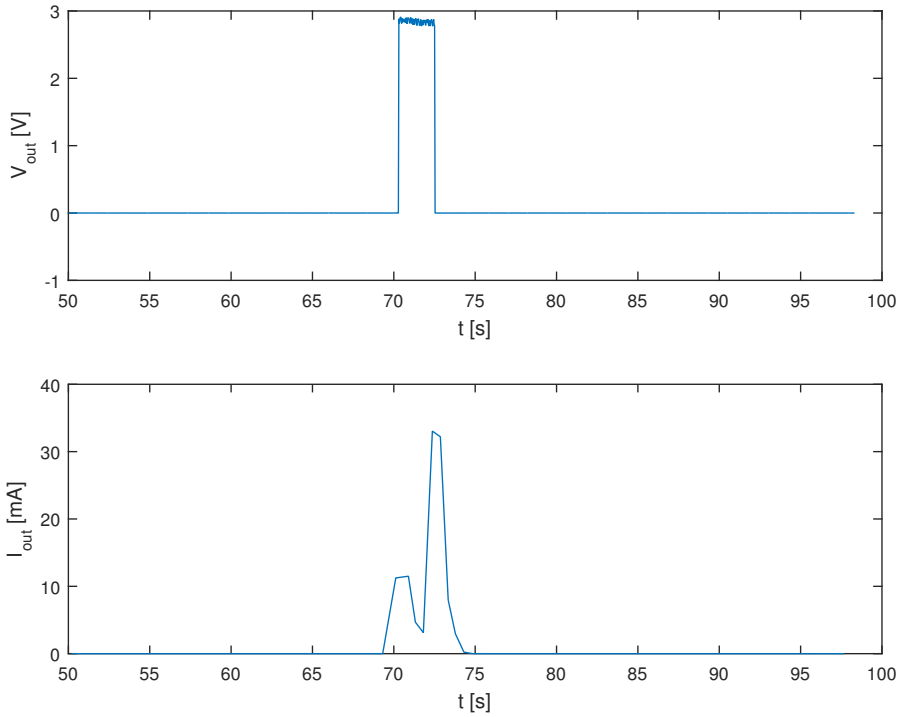

Figure 7-5
Startup with switched output voltage

Component	Current [mA]
Sensor node (avg.)	0.148
DC-DC converter	0.001
Output capacitor leakage	0.004
Storage capacitor leakage	0.140

Table 7-2: Average power consumption

is connected when the output voltage reaches about $3\,\mathrm{V}$. The high current consumed by the buzzer mens that the output voltage subsequently drops low enough that the output gets turned off again. While this improves over the case with no switch, where the system gets caught in an incorrect operating state and drains all energy, this means that the system is not able to start correctly with depleted storage.

To achieve startup even with a depleted storage capacitor, a supervising circuit would have to be implemented, which only starts the sensor node when sufficient energy is available in storage.

7.3 Storage

This section will focus on the ability of the storage capacitors to allow long term operation, and not discuss the influence of leakage on system efficiency. To test this, the storage was first charged to a voltage of $5.13\,\mathrm{V}$, with the sensor node already attached, to make sure that the startup, which takes more power than usual operation, does not influence the runtime measurement. The local testbed at the ETZ building was used to achieve realistic operating conditions, and to measure the time stamp of the last message the node was able to send.

Based on the model, the prototype, with a storage capacity of $30\,\mathrm{F}$ should achieve a runtime of 60 hours. The measured runtime of the system was found to be only 30 hours. As the power requirement of the sensor node is well known from operation, it is assumed that this mismatch is due to poor modeling of the leakage current. [18] proposes a more detailed supercapacitor model which could better explain the behavior of the storage capacitor. Another issue with this design is the high voltage applied to the capacitor. The power loss due to leakage is a much bigger problem at high voltages, and this could be avoided with the use of multiple low voltage capacitors in series.

Table 7-2 shows an overview of the power consumption of the system, where it is clearly visible that, in the prototype system, about fifty percentage of the energy is lost to leakage.

7.4 Summary

Evaluation of the prototype has shown that the use of a bipolar harvester means that the conversion efficiency is greatly reduced, which is only partly recovered by the ability to harvest both during the day and the night. The special requirements

of the sensor node, namely the buzzer which indicates system startup, also make it necessary to integrate a special startup circuit, which makes sure that the system can start properly, and does not unnecessarily waste energy. Measurement of the storage capacitor also demonstrates that the supercapacitor cannot be modeled as a normal capacitor with sufficient accuracy, and a more sophisticated model has to be used.

8

Conclusion

8.1 Conclusion

First, we performed a characterization of the temperature gradients occurring at the Matterhorn, and described both short- and long-term changes in the available temperature gradient. Then, a model was developed to perform an initial evaluation of the feasibility of bipolar energy harvesting. Based on this, an prototype of the harvesting system was designed and evaluated. Testing of the prototype has shown that the efficiency of the bipolar harvester is lower than expected. The results also show that bipolar harvesting is not as efficient as initially assumed. While it allows harvesting from both gradients, the design of the converter means that it less efficient, especially when exposed to higher voltage inputs. The discussed prototype is also clearly not able to provide enough energy for perpetual operation without use of a primary, non-rechargeable battery. To achieve this, further work is required in all areas of the system. The following section discusses some possible directions.

8.2 Future Work

The model used in this thesis assumes that the temperature of the sensor node can be used to estimate the heatsink temperature in the energy harvesting system. It is also assumed that the temperature difference over the TEG will be half to the total temperature difference between rock surface and rock interior. Optimizing and evaluating this part of the system with a thermal prototype system could offer more information over the actually achievable temperature gradients.

The low temperature environment of the high alpine region poses special requirements to storage technologies, and limits their use. The use of a dedicated storage management circuit could allow the use of components with less leakage, and greatly increase system uptime.

In the discussed prototype, the harvesting system is not very well integrated with the actual sensor node. An updated sensor node designed with energy harvesting in mind could increase efficiency by getting rid of duplicate components, such as

voltage regulators, by choosing components which can work with the output voltage of the DC-DC converter.

A

Prototype schematics

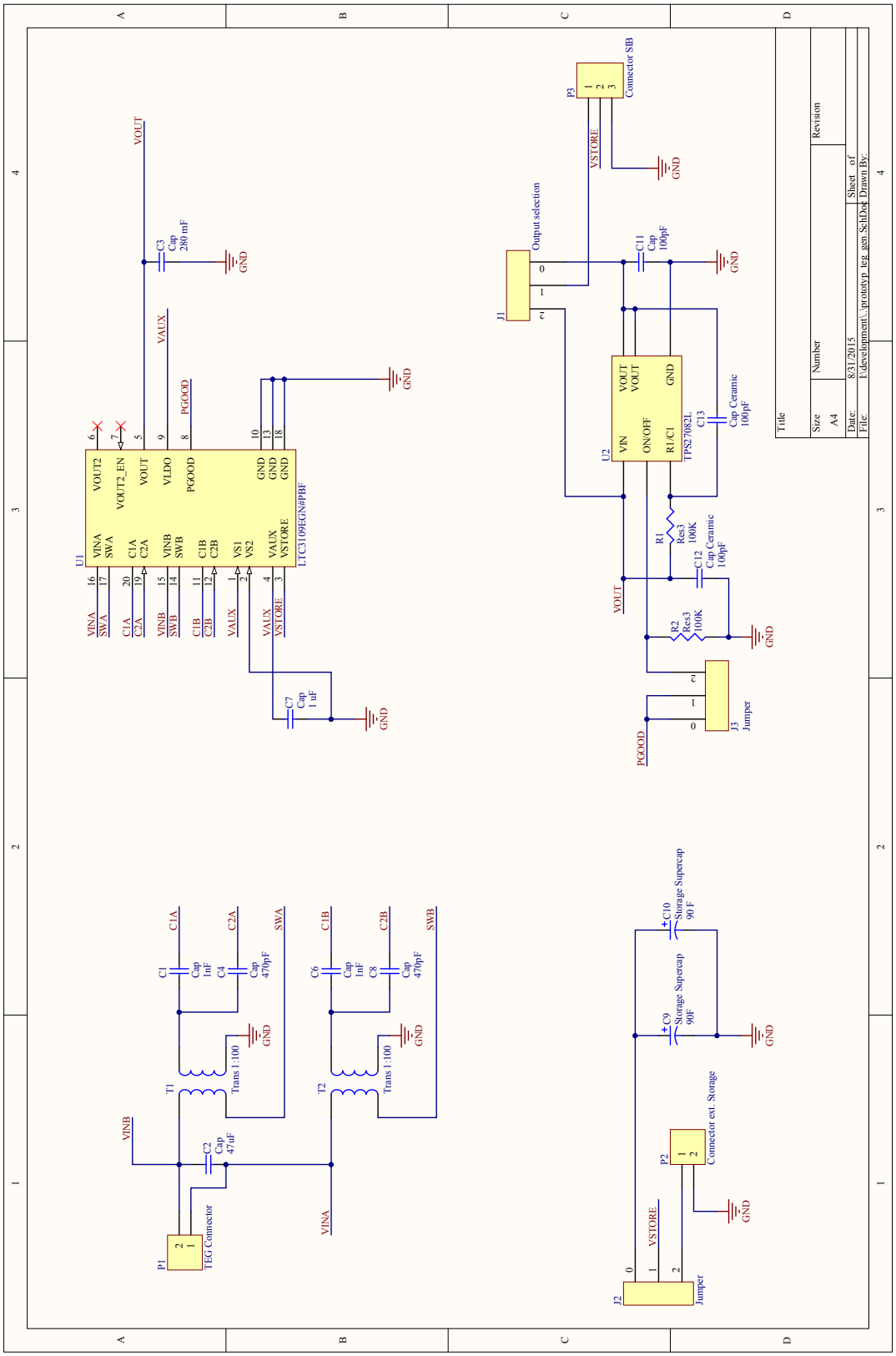
U1
LTC3109EGN#PBF
VOUT2
VOUT2_EN
VOUT
VLDO
PGOOD
VINA
SWA
C1A
C2A
VINB
SWB
C1B
C2B
VS1
VS2
VAUX
VSTORE
GND
C3
Cap
280 mF
C7
Cap
1 uF
U2
TPS27082L
VIN
ON/OFF
R1/C1
C13
Cap Ceramic
100pF
C11
Cap
100pF
R1
Res3
100K
C12
Cap Ceramic
100pF
R2
Res3
100K
J1
Output selection
J3
Jumper
P3
Connector SB
C1
Cap
1uF
C4
Cap
470pF
C6
C8
T1
T2
Trans 1:100
C2
Cap
47uF
P1
TEG Connector
C10
Storage Supercap
90 F
C9
Storage Supercap
90F
P2
Connector ext. Storage
J2
Jumper
Title
Size
A4
Number
Revision
Date:
8/31/2015
Sheet of
File:
I:\development\..\prototyp_teg_gen.SchDoc
Drawn By:

B

Task description

ETH
Eidgenössische Technische Hochschule Zürich
Swiss Federal Institute of Technology Zurich

Computer Engineering and Networks Lab

ETZ G 75
CH-8092 Zurich

Dr. Jan Beutel
Gloriastr. 35
+41-44-6327032
+41-44-6321035
beutel@tik.ee.ethz.ch
www.tik.ee.ethz.ch/~beutel

MASTERARBEIT
Für
Dominik Böhi

Betreuer: Jan Beutel
Stellvertreter: Reto Da Forno

Ausgabe: 23. März 2015
Abgabe: 23. September 2015

Thermal Energy Scavenging for WSNs

Das PermaSense Projekt befasst sich mit der Beobachtung physikalischer Parameter des Permafrostes in den Schweizer Alpen. Zu diesem Zweck entwickelt und betreibt das Projekt verschiedene Messsysteme. In diesem Projekt soll für die drahtlosen Sensoren ein System zur Energiegewinnung und Speicherung entwickelt werden das diese Sensoren unabhängig von einer Batterie als Energiequelle macht. Zu diesem Zweck soll ein Thermoelektrischer Generator verwendet werden der den regelmäßig stattfindenden Wärmefluss zwischen Felswand und Atmosphäre bzw. Strahlung in elektrische Energie umwandelt. Im Rahmen dieser Masterarbeit soll ein geeignetes Systemkonzept entwickelt sowie ein Prototyp realisiert werden. Neben der Arbeit an Konzept und Realisierung sind Messungen zur Charakterisierung und Dimensionierung sowie geeignete Modellierungen integraler Bestandteil der Arbeit.

Aufgabenstellung

- Erstellen Sie einen Projektplan und legen Sie Meilensteine sowohl zeitlich wie auch thematisch fest. Erarbeiten Sie in Absprache mit dem Betreuer ein Pflichtenheft.
- Machen Sie sich mit den relevanten Arbeiten im Bereich (Thermal) Energy Harvesting vertraut. Führen Sie eine Literaturrecherche durch. Suchen Sie gezielt nach relevanten Publikationen. Prüfen Sie welche Ideen/Konzepte Sie aus diesen Lösungen verwenden können. Positionieren Sie Ihre Arbeit in diesem Kontext.
- Erstellen Sie eine Übersicht der Anforderungen des zu entwickelnden Thermoelektrischen Generators bzw. die Energiespeicherung um ein PermaSense Sensor Interface Board (SIBv2) und TinyNode zu betreiben. Leiten Sie hieraus eine Funktionsspezifikation ab.
- Zur Evaluierung des Systemdesigns bzw. einzelner Systemkomponenten sind geeignete Modelle bzw. Testaufbauten zu entwickeln und einzusetzen.
- Entwerfen Sie auf Basis der Funktionsspezifikation ein Systemdesign für Generator, DC/DC Konvertierung, Energiespeicherungen sowie die Anbindung an das PermaSense SIBv2. Der Entwurf beinhaltet die Auswahl der Komponenten,

Schaltungsdesign und Mechanisches Design. Begründen Sie ihre Architekturentscheide wo immer möglich quantitativ.
- Implementieren Sie einen lauffähigen Prototyp. Charakterisieren sie die Systemeigenschaften und Performance dieses Prototyps anhand von Messungen.
- Achten Sie darauf, dass die angestrebte Lösung auch in der Praxis anwendbar ist.
- Weiterhin soll im Verlauf der Arbeit eine technische Dokumentation des Gesamtsystems erstellt werden.
- Dokumentieren Sie Ihre Arbeit sorgfältig mit einem Vortrag, einer kleinen Demonstration, sowie mit einem Schlussbericht.
- Optional: Optimierung des Energieverbrauchs des PermaSense SIBv2.
- Optional: Integration eines Wärmeflusssensors an ein PermaSense SIBv2 zur in-situ Charakterisierung.
- Optional: Test des Prototyps in einem geeigneten Feldversuch am Matterhorn.

Durchführung der Masterarbeit

Allgemeines
- Der Verlauf des Projektes soll laufend anhand des Projektplanes und der Meilensteine evaluiert werden. Unvorhergesehene Probleme beim eingeschlagenen Lösungsweg können Änderungen am Projektplan erforderlich machen. Diese sollen dokumentiert werden.
- Sie verfügen über PCs mit Linux/Windows für Softwareentwicklung und Test. Für die Einhaltung der geltenden Sicherheitsrichtlinien der ETH Zürich sind Sie selbst verantwortlich. Falls damit Probleme auftauchen wenden Sie sich an Ihren Betreuer.
- Stellen Sie Ihr Projekt zu Beginn der Semesterarbeit in einem Kurzvortrag vor und präsentieren Sie die erarbeiteten Resultate am Schluss im Rahmen des Institutskolloquiums Ende Semester.
- Besprechen Sie Ihr Vorgehen regelmäßig mit Ihren Betreuern. Verfassen Sie dazu auch einen kurzen wöchentlichen Statusbericht (email).

Abgabe
- Geben Sie zwei Exemplare des Berichtes spätestens am 23. September 2015 dem betreuenden Assistenten oder seinem Stellvertreter ab. Diese Aufgabenstellung soll im Bericht eingefügt werden genauso wie das unterschriebene Unterschriftenblatt „Plagiat" des Rektorats. Die Entsprechenden Richtlinien des Rektorats sind einzuhalten.
- Räumen Sie Ihre Rechnerkonten soweit auf, dass nur noch die relevanten Quellcode- und Binärdateien, Konfigurationsdateien, benötigte Verzeichnisstrukturen usw. bestehen bleiben. Der Programmcode sowie die Dateistruktur sollen ausreichend dokumentiert sein. Eine spätere Anschlussarbeit soll auf dem hinterlassenen Stand aufbauen können.

C

Declaration of Originality

Bibliography

[1] W. K. Seah, Y. Tan, and A. T. Chan, "Research in Energy Harvesting Wireless Sensor Networks and the Challenges Ahead," in *Autonomous Sensor Networks*, D. Filippini, Ed. Springer Berlin Heidelberg, 2013, pp. 73–94.

[2] C. Wu, "Analysis of waste-heat thermoelectric power generators," *Applied Thermal Engineering*, vol. 16, no. 1, pp. 63–69, Jan. 1996.

[3] A. Moser, L. Rendler, M. Kratschmer, and P. Woias, "Transient model for thermoelectric generator systems harvesting from the natural ambient temperature cycle," *Proceedings of PowerMEMS*, 2010.

[4] A. Agbossou, Q. Zhang, G. Sebald, and D. Guyomar, "Solar micro-energy harvesting based on thermoelectric and latent heat effects. Part I: Theoretical analysis," *Sensors and Actuators A: Physical*, vol. 163, no. 1, pp. 277–283, 2010.

[5] Q. Zhang, A. Agbossou, Z. Feng, and M. Cosnier, "Solar micro-energy harvesting based on thermoelectric and latent heat effects. Part II: Experimental analysis," *Sensors and Actuators A: Physical*, vol. 163, no. 1, pp. 284–290, Sep. 2010.

[6] J. Beutel, S. Gruber, A. Hasler, R. Lim, A. Meier, C. Plessl, I. Talzi, L. Thiele, C. Tschudin, M. Woehrle, and M. Yuecel, "PermaDAQ: A scientific instrument for precision sensing and data recovery in environmental extremes," *2009 International Conference on Information Processing in Sensor Networks*, 2009.

[7] H. Dubois-Ferrière, L. Fabre, R. Meier, and P. Metrailler, "TinyNode," in *Proceedings of the fifth international conference on Information processing in sensor networks - IPSN '06*. New York, New York, USA: ACM Press, Apr. 2006, p. 358.

[8] P. Douglas, "Thermoelectric energy harvesting," in *ICT - Energy - Concepts Towards Zero - Power Information and Communication Technology*, G. Fagas, L. Gammaitoni, P. Douglas, and G. A. Berini, Eds. InTech, 2014, ch. 4.

[9] S. Priya and D. J. Inman, "Energy harvesting technologies," *Energy Harvesting Technologies*, pp. 1–517, 2009.

[10] *bq25504 Datasheet*, Texas Instruments, 2014, revision B.

[11] *LTC3109 Datasheet*, Linear Technology, 2013, revision B.

[12] *BestCap® Ultra-low ESR High Power Pulse Supercapacitors*, AVX.

[13] "Lithum ion capacitors - whitepaper," Taiyo Yuden, accessed 18.09.2015. [Online]. Available: http://www.yuden.co.jp/include/english/solutions/lic/LIC_White_Paper_Final.pdf

[14] *GM200-71-14-16 - Datasheet*, European Thermodynamics Limited, accessed 18.09.2015. [Online]. Available: http://www.europeanthermodynamics.com/products/datasheets/GM200-71-14-16(2).pdf

[15] *TEG 127-175-25 - Datasheet*, thermalforce, accessed 18.09.2015. [Online]. Available: http://thermoelectrics.de/de/product/thermogenerator/TG127-175-25c.pdf

[16] *TEG 241-150-29 - Datasheet*, thermalforce, accessed 18.09.2015. [Online]. Available: http://thermoelectrics.de/de/product/thermogenerator/TG241-150-29c.pdf

[17] *TEG 127-200-28 - Datasheet*, thermalforce, accessed 18.09.2015. [Online]. Available: http://thermoelectrics.de/de/product/thermogenerator/TG127-200-28k.pdf

[18] A. Weddell, G. V. Merrett, T. Kazmierski, and B. Al-Hashimi, "Accurate supercapacitor modeling for energy harvesting wireless sensor nodes," *Circuits and Systems II: Express Briefs, IEEE Transactions on*, vol. 58, no. 12, pp. 911–915, 2011.